JACS
JOURNAL OF THE AMERICAN CHEMICAL SOCIETY

Article

pubs.acs.org/JACS

# In Vitro and Mechanistic Studies of an Antiamyloidogenic Self-Assembled Cyclic D,L-α-Peptide Architecture

Michal Richman,[‡,§] Sarah Wilk,[‡,§] Marina Chemerovski,[‡] Sebastian K. T. S. Wärmländer,[†] Anna Wahlström,[†] Astrid Gräslund,[†] and Shai Rahimipour*[,‡]

[‡]Department of Chemistry, Bar-Ilan University, Ramat-Gan 5290, Israel

[†]Department of Biochemistry and Biophysics, Arrhenius Laboratories, Stockholm University, S-106 91 Stockholm, Sweden

Supporting Information

**ABSTRACT:** Misfolding of the Aβ protein and its subsequent aggregation into toxic oligomers are related to Alzheimer's disease. Although peptides of various sequences can self-assemble into amyloid structures, these structures share common three-dimensional features that may promote their cross-reaction. Given the significant similarities between amyloids and the architecture of self-assembled cyclic D,L-α-peptide, we hypothesized that the latter may bind and stabilize a nontoxic form of Aβ, thereby preventing its aggregation into toxic forms. By screening a focused library of six-residue cyclic D,L-α-peptides and optimizing the activity of a lead peptide, we found one cyclic D,L-α-peptide (**CP-2**) that interacts strongly with Aβ and inhibits its aggregation. In transmission electron microscopy, optimized thioflavin T and cell survival assays, **CP-2** inhibits the formation of Aβ aggregates, entirely disassembles preformed aggregated and fibrillar Aβ, and protects rat pheochromocytoma PC12 cells from Aβ toxicity, without inducing any toxicity by itself. Using various immunoassays, circular dichroism spectroscopy, photoinduced cross-linking of unmodified proteins (PICUP) combined with SDS/PAGE, and NMR, we probed the mechanisms underlying **CP-2**'s antiamyloidogenic activity. NMR spectroscopy indicates that **CP-2** interacts with Aβ through its self-assembled conformation and induces weak secondary structure in Aβ. Upon coincubation, **CP-2** changes the aggregation pathway of Aβ and alters its oligomer distribution by stabilizing small oligomers (1−3 mers). Our results support studies suggesting that toxic early oligomeric states of Aβ may be composed of antiparallel β-peptide structures and that the interaction of Aβ with **CP-2** promotes formation of more benign parallel β-structures. Further studies will show whether these kinds of abiotic cyclic D,L-α-peptides are also beneficial as an intervention in related in vivo models.

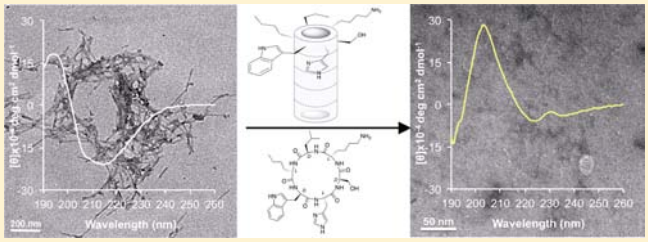


## INTRODUCTION

An increasing body of evidence suggests that protein misfolding and aggregation is the fundamental cause of many amyloidogenic diseases. The deposition of proteins in the form of amyloid fibrils and plaques is the characteristic feature of more than 20 degenerative conditions affecting either the central nervous system or a variety of peripheral tissues.[1] These conditions include Alzheimer's, Parkinson's, and Huntington's diseases, and type II diabetes.

It is well established that misfolded proteins are not normally biologically active; nevertheless, they are present in a dynamic equilibrium between monomeric and oligomeric forms that can lead to an aggregated state that is toxic to cells. At the present time, the link between amyloid formation and the diseases they cause is based mainly on a large number of biochemical and genetic studies.[2] However, intense debate surrounds the specific natures and structure of the pathogenic species and the molecular basis for their ability to damage cells.[1,3−5]

For Alzheimer's disease (AD), the oligomerization of amyloid beta (Aβ) to soluble oligomers and their accumulation in the brain are believed to be the primary pathogenic events that lead to synaptic loss and selective neuronal cell death.[3,6,7] Aβ is a short amyloidogenic polypeptide (40−43 amino acids) generated from the proteolytic cleavage of the transmembrane amyloid precursor protein (APP). Reducing Aβ levels in the brain by recruiting the immune system[8,9] or inhibiting Aβ aggregation via agents that interfere with its self-assembly[10,11] are promising strategies for AD therapy.[12] However, Aβ can adopt different structural conformations depending on the environment. Moreover, although the toxic species in AD is hypothesized to be soluble low molecular weight (LMW) Aβ oligomers, the overall structure of these oligomers and the conformation of Aβ within these species are still unknown. This dearth of structural information clearly makes rational design of therapeutic agents a challenging task.

Recent studies have shown that pathogenic amyloids share common structural features despite being composed of different proteins and amino acids. Indeed, a large degree of β-structure is evident in different aggregated proteins, even when the monomeric peptide or protein is substantially disordered or rich in α-helical regions.[13,14] Moreover, soluble

**Received:** October 11, 2012
**Published:** January 29, 2013

   dx.doi.org/10.1021/ja310064v | J. Am. Chem. Soc. 2013, 135, 3474−3484

**Scheme 1. Structural Similarities between the Self-Assembly Process of (A) Aβ Peptide and (B) Cyclic D,L-α-Hexapeptide[a]**

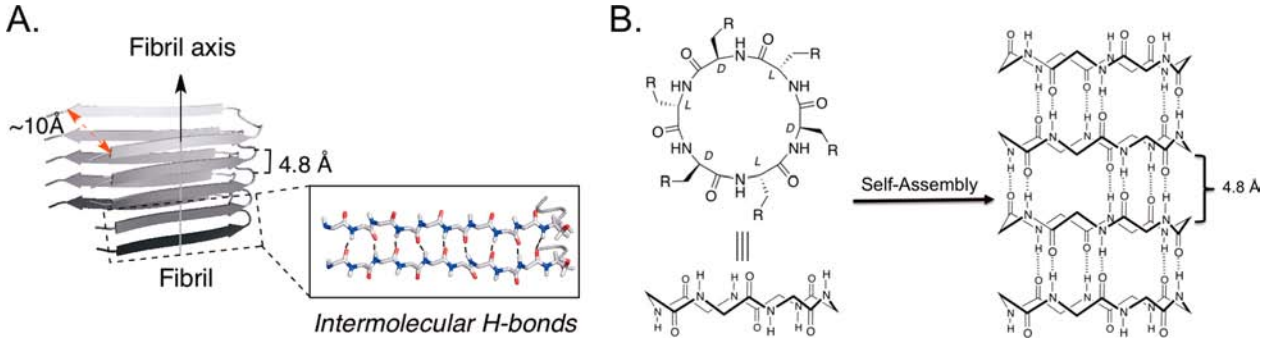


[a]For clarity, all of the side-chains have been omitted. The amyloid structure is adapted from Lührs et al., while the structure of the cyclic peptide is based on the known core structure of cyclic D,L-α-peptide octamer.[26,27]

aggregates of various amyloidogenic proteins, such as insulin, islet amyloid polypeptide (IAPP, also called amylin), and α-synuclein, are equally recognized by polyclonal antibodies raised against prefibrillar assemblies of Aβ peptides.[15] Overall, these results suggest that amyloid cytotoxicity may arise from some common aspect of the supramolecular structure of the aggregates rather than from specific sequences or characteristics of their amino acid composition.

The strong structural similarities between the amyloidogenic protein aggregates may also be related to their cross-reactivity, as may be expected in a dynamic and reversible self-assembly system.[16] For example, Aβ interacts specifically with various amyloidogenic proteins, including tau, α-synuclein, transthyretin, and IAPP, and modulates their aggregation.[17−20] On the basis of these interactions, Kapurniotu and co-workers developed novel IAPP-mimics that inhibit the aggregation and toxicity of Aβ, insulin, and IAPP.[17,21] Cross-reactivity between Aβ and IAPP may also be responsible for the increased incidence of Alzheimer's disease (AD) among patients with type II diabetes.[22]

Consistently with these conclusions, prefibrillar assemblies of different proteins have been shown to interact similarly with synthetic phospholipid bilayers and with cell membranes and to cause their destabilization.[23,24] In most cases, interactions between a misfolded protein and a membrane occur via a two-step mechanism in which positively charged residues electrostatically interact with negatively charged or polar lipid head groups, and then hydrophobic regions insert into the membrane. This mode of activity resembles that of membrane-active antimicrobial peptides forming pore-like assemblies on a membrane.[25] Increased generation of reactive oxygen species (ROS) and indirect activation of microglia and immune cells by Aβ species have been also suggested as possible mechanisms of amyloid toxicity.[5]

Remarkably, the structural and biochemical characteristics of amyloids strikingly resemble those ofcyclic D,L-α-peptide nanotubes (Scheme 1).[26,27] These supramolecular structures are generated from the self-assembly of simple cyclic peptides comprising an even number of alternating D- and L-α amino acids that can form flat and ring-shaped conformations. Under conditions that favor hydrogen-bond formation, cyclic D,L-α-peptides stack on top of each other to form hollow β-sheet-like tubular structures that can act as effective ion channels.[27,28] The hydrogen bonds in such structures run parallel to the axis of the nanotubes and separate the cyclic peptides from each other by ∼4.8 Å. A similar intermolecular distance is also evident in the β-strands of the amyloids (Scheme 1). Accordingly, the structure of cyclic D,L-α-peptides, similarly to that of amyloids, is dictated mainly by hydrogen bonding in the backbone, which, in the case of cyclic D,L-α-peptide nanotubes, stems from an alternating D- and L-α-amino acid configuration. Cyclic D,L-α-peptides can exhibit diverse biological activities, including antibacterial and antiviral properties.[29,30] Interestingly, the mode of action of antibacterial cyclic D,L-α-peptides shares some similarity with that of the amyloids, in that it involves membrane interaction and perturbation via the formation of nonspecific ion channels or pores that leads to the loss of membrane integrity and cytotoxicity.[24,29]

The strong similarities between amyloids and self-assembled cyclic D,L-α-peptides led us to hypothesize that appropriately designed cyclic D,L-α-peptides may cross-react with Aβ through a complementary sequence of hydrogen-bond donors and acceptors to modulate Aβ aggregation and toxicity. In this study, we report the discovery of a novel antiamyloidogenic family that is based on abiotic cyclic D,L-α-peptide architectures. By using a wide range of chemical, biophysical, and biochemical techniques, we demonstrate that these cyclic peptides can inhibit the formation of toxic aggregates and can disassemble preformed Aβ fibrils by interacting with several regions of the soluble Aβ sequence and inducing structural changes to unfolded Aβ. Moreover, the cyclic peptides are not toxic and protect pheochromocytoma PC12 cells from Aβ toxicity.

## ■ MATERIALS AND METHODS

**Peptide Synthesis.** Peptide analogues were synthesized by solid-phase peptide synthesis, employing the common Fmoc strategy. Detailed synthetic procedures are provided in the Supporting Information.

**Synthesis of Cyclic D,L-α-Peptide Library.** The cyclic peptide library was synthesized on trityl chloride-loaded polystyrene macrobeads (500−560 μm; Peptides International, Louisville, KY) as described in the Supporting Information, using the split and pool methodology.[31] Fmoc-Lys-OAllyl was used as the first anchored amino acid. Coupling reactions were carried out with 5 equiv of diisopropylcarbodiimide/hydroxybenzotriazole (DIC/HOBt) in 1-methyl-2-pyrrolidone (NMP). Completion of the reaction was monitored by bromophenol dye.[32] Following assembly of the linear sequence, the allyl protecting group was removed under an Ar atmosphere by treating the resin with $Pd(PPh_3)_4$ (0.3 equiv) and $PhSiH_3$ (10 equiv) in $CH_2Cl_2$ for 4 h. This procedure was repeated to ensure complete removal of the allyl protecting group. The resin was washed with a solution of 1% sodium dimethylthiocarbamic acid in dimethylformamide (DMF) and then with 1% *N*,*N*-diisopropylethylamine (DIEA) in DMF. The linear peptide was then cyclized while still


dx.doi.org/10.1021/ja310064v | J. Am. Chem. Soc. 2013, 135, 3474−3484

on the resin using a solution of benzotriazol-1-yl-oxytripyrrolidinophosphonium hexafluorophosphate (PyBOP), HOBt, and DIEA (5, 5, and 15 equiv) in NMP for 6 h. This procedure was repeated twice. Methanol dried macrobeads were then individually arrayed into discrete wells of a 96-well polypropylene plate and treated with a mixture (100 $\mu$L) of trifluoroacetic acid:triisopropylsilane:water (95:2.5:2.5) for 2 h. The volatiles were removed by reduced pressure using a SpeedVac system (ThermoSavant, Holbrook, NY). Finally, the crude cyclic peptides were dissolved in dimethyl sulfoxide (DMSO) and diluted with $H_2O$ to afford a stock peptide solution of approximately 1 mM (based on resin loading) in 10% DMSO.

**Thioflavin T (ThT) Aggregation Assay.** A$\beta$40 and A$\beta$42 were purchased from Sigma and stored as lyophilized powder at −80 °C until used. To ensure the monomeric state of the peptide, the Zagorski method was employed.[33] The inhibitory activity of the cyclic peptides on A$\beta$ aggregation was determined in black 96-well flat-bottom plates according to Richman et al.[34] Full experimental details and procedures for screening of the library are given in the Supporting Information.

**Seeding Assay.** A$\beta$40 fibrils were prepared at a concentration of 100 $\mu$M by aging monomeric A$\beta$40 (100 $\mu$M, in 50 mM phosphate buffered saline; PBS) for 5 days at 37 °C, and were stored at −80 °C until used. For the seeding experiments, A$\beta$ fibrils (5% v:v based on the amount of monomeric A$\beta$40) were sonicated in an ice−water bath for 5 min and incubated for 5 min with vehicle or **CP-2** (100 $\mu$M) in PBS-Gly buffer (50 mM) containing ThT (18 $\mu$M). Monomeric A$\beta$40 (10 $\mu$M) was then added to the wells, and the plates were sealed with clear polyolefin foil and incubated at 37 °C. The fluorescence of amyloid-bound ThT was then measured for 48 h using a plate reader (Infinite M200, Tecan, Switzerland) at excitation and emission wavelengths of 430 and 492 nm, respectively.

**Transmission Electron Microscopy (TEM) Analysis.** Samples were prepared for TEM studies by spotting aliquots (5 $\mu$L) of the aggregation assay onto glow-discharged, carbon-coated Formvar/copper grids (SPI supplies, West Chester, PA). The samples were then blotted with a filter paper and allowed to dry for 20 min. The samples were negatively stained with 2% uranyl acetate in water (5 $\mu$L) for 30 s, blotted with filter paper, and dried for an additional 20 min. Samples were then analyzed by a Tecnai G2 TEM (FEI TecnaiTM G2, Hillsboro, OR) operated at 120 kV.

**Circular Dichroism (CD) Spectroscopy.** CD measurements were carried out using a Chirascan spectrometer (Applied Photophysics, UK). Samples were prepared in a manner similar to that for the ThT aggregation assay and analyzed daily. Measurements were performed at room temperature in a 2 mm optical path length cell without dilution, and the spectra were recorded from 260−190 nm with a step size and a bandwidth of 1 nm. The spectra are the average of three measurements after background subtraction.

**Photo-Induced Cross-Linking of Unmodified Proteins (PICUP).** PICUP was performed according to the protocol of Bitan et al.[35] Samples were prepared for PICUP in a manner similar to that for the aggregation assay and were analyzed daily. The concentrations of A$\beta$40 and of the cyclic D,L-$\alpha$-peptide **CP-2** in all samples were 50 and 500 $\mu$M, respectively. After each time interval, samples (18 $\mu$L) were mixed with ammonium persulfate (APS; 1 $\mu$L, 20 mM) and [tris(2,2′-bipyridyl)-ruthenium(II)] (1 $\mu$L, 1 mM), both in PBS (10 mM). The mixture was then irradiated for 30 s using a 150 W lamp positioned 15 cm from the bottom of the reaction tube. Cross-linking reactions were quenched immediately with 10 $\mu$L of sample buffer (Invitrogen) containing 5% $\beta$-mercaptoethanol. Samples were then analyzed using a 10−20% tricine SDS-poly acrylamide gel and visualized by the silver stain method.

**Dot Blot Assay.** Monomeric A$\beta$40 and A$\beta$42 (50 $\mu$M) were incubated for different intervals in the absence or presence of **CP-2** (500 $\mu$M) in PBS and kept at −80 °C until analyzed. Samples (5 $\mu$L) were then spotted onto nitrocellulose membranes (0.2 $\mu$m) and dried at room temperature. The membranes were then blocked for 1 h with 5% nonfat milk in Tris buffered saline (TBS, 10 mM) containing 0.01% Tween 20 (TBST), washed three times (5 min) with TBST, and incubated at 4 °C overnight with polyclonal antibody A11 (Millipore) at 1:1000 in 0.5% nonfat milk in TBST. The membranes were washed with TBST and incubated for 1 h with horseradish peroxidase (HRP) conjugated antirabbit IgG at 1:5000 in 0.5% nonfat milk in TBST at room temperature. The blots were then washed five times with TBST and developed using the ECL reagent kit (Pierce). The same membranes were stripped as described,[15] washed five times with TBST, blocked for 1 h with 5% nonfat milk, and incubated at 4 °C overnight with 6E10 antibody (Covance) at 1:1000 in 0.5% nonfat milk in TBST. The TBST-washed membranes were then reacted for 1 h with HRP conjugated antimouse IgG (1:10 000) and developed with ECL.

**ELISA Assay.** A$\beta$ oligomer-specific antibody (OMAB, Agrisera, Sweden) at 2 $\mu$g mL$^{-1}$ in PBS was adsorbed overnight onto Nunc-Immuno MaxiSorp plates (Nunc, Denmark) at 4 °C. Wells were then blocked for 1 h at 4 °C with 5% nonfat milk in PBS containing 0.1% Tween 20 (PBST), washed three times with PBST, and incubated for 45 min with A$\beta$ samples (50 $\mu$M) that had been incubated for different intervals in the absence or presence of **CP-2** (500 $\mu$M) in PBS. Samples were diluted 1:50 with PBS prior to the assay. The treated wells were washed three times with PBST and exposed to the 6E10 antibody (1:1000 dilution in 5% nonfat milk in PBST) for 1 h at room temperature. The wells were washed three times with PBST, incubated with an antimouse HRP-conjugated IgG (1:10 000 dilution in 5% nonfat milk in PBST) for 1 h, and developed by 3,3′,5,5′-tetramethylbenzidine (TMB). The reaction was stopped with 1 N $H_3PO_4$, and the absorbance of each well was measured at 450 nm using a plate reader.

**Cell Culture Experiments.** PC12 cells were maintained in low-glucose Dulbecco's Modified Eagle Medium (DMEM) supplemented with horse serum (10%) and fetal bovine serum (FBS; 5%), L-glutamine, penicillin, and streptomycin in a 5% $CO_2$ atmosphere at 37 °C. To evaluate the effect of the cyclic D,L-$\alpha$-peptides on A$\beta$-induced toxicity, A$\beta$40 (200 $\mu$M) and A$\beta$42 (400 $\mu$M) were aged for 48 h in the absence or presence of the cyclic peptides (up to a 10-fold mole to mole excess of **CP-2** to A$\beta$) in 5% DMSO in PBS in a total volume of 50 $\mu$L. Prior to the addition of the samples to the cells, the aggregation of A$\beta$40 in each sample was confirmed by ThT assay. On the day of the experiment, the medium was replaced with fresh medium (90 $\mu$L), and the aged samples (10 $\mu$L) were then diluted by a factor of 10 in the medium. Control wells received PBS (10 $\mu$L) containing 0.25% DMSO (100% cell viability) or 2% SDS solution as a positive control to kill all of the cells (0% cell viability). Cells were incubated for an additional 24 h, and cell viability was then determined by the 3-(4,5-dimethylthiazol-2-yl)-2,5-diphenyltetrazolium bromide (MTT) assay. Each experiment was performed in quadruplicate and repeated three times.

**NMR Spectroscopy.** NMR experiments were carried out with Bruker 600 and 700 MHz instruments. Unlabeled and $^{15}$N-labeled A$\beta$40 peptide was purchased from AlexoTech AB (Sweden) and prepared in $D_2O$ or $D_2O$:$H_2O$ (1:9; v:v) according to a previously published protocol to obtain monomeric NMR samples in the 50−75 $\mu$M range.[36] A stock solution of the cyclic peptide was prepared by dissolving it in $D_2O$:DMSO-$d_6$ (1:1; v:v) to obtain a peptide concentration of 17.5 mM. The concentration of the peptide was determined spectroscopically at 280 nm, using an extinction coefficient of 5690 M$^{-1}$ cm$^{-1}$. NMR samples were prepared using a 10 mM sodium phosphate buffer at pD 7.4 that contained a small amount of 4,4-dimethyl-4-silapentane-1-sulfonic acid (DSS) for spectrum reference purposes. NMR spectra were recorded at +5 °C both as 2D $^1$H−$^{15}$N-HSQC spectra and in a 1D format using excitation sculpting water suppression. The $^1$H−$^{15}$N-HSQC spectrum of A$\beta$40 was assigned according to our previously published assignment.[36]

## RESULTS AND DISCUSSION

The biological activity of most bioactive cyclic D,L-$\alpha$-peptides is sensitive to minor amino acid modifications.[29,30] For this reason, and because of the large potentially bioactive sequence space within cyclic D,L-$\alpha$-peptides that can interact with A$\beta$, we employed the "one-bead-one-compound" combinatorial approach[31] to select peptides that could potentially cross-react

with A$\beta$ and inhibit its aggregation and toxicity. To probe the general topological requirements for antiamyloidogenic activity, representative amino acids with different functional side chains, including positively (Lys) and negatively (Glu) charged, neutral hydrophilic (Ser), neutral hydrophobic (Leu), and aromatic (Trp, His) amino acids, were introduced to five positions of the cyclic D,L-$\alpha$-peptide hexamer. Position one was fixed with Lys to allow the peptides to be attached to a solid support via the free amine side chain and cyclized through head-to-tail cyclization. These amino acids were chosen to provide manageable library diversity and a broad representation of sequence−activity relationships. Figure 1 schematically depicts the synthesized

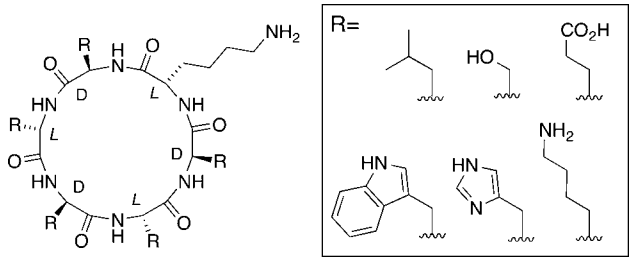


**Figure 1.** Schematic representation of the 7776 member cyclic D,L-$\alpha$-peptide library that was synthesized and screened for antiamyloidogenic peptides.

library and its corresponding diversity. The library was prepared on macrobeads using standard solid-phase peptide synthesis (SPPS) techniques, using the Fmoc methodology. Following the synthesis of the linear peptides, they were cyclized on the solid support as described in Scheme S1.

Next, we screened 500 randomly chosen members of the library for their antiamyloidogenic activity. Each of the 500 candidates (10 $\mu$M) was screened for its ability to inhibit the aggregation of A$\beta$40 (10 $\mu$M). The optimized ThT assay was used to probe the formation of amyloid aggregates, in which a large increase in ThT fluorescence is generated upon binding of ThT to aggregated A$\beta$.[37] The sequences of two cyclic peptides that were found to show antiamyloidogenic activity also at 3 $\mu$M were then determined by tandem mass spectrometry ($MS^2$).[38] The antiamyloidogenic activities of the synthesized hits were revalidated at several concentrations. Ac-KLVFF-$NH_2$ was used as a positive control with a known inhibitory effect on A$\beta$ aggregation.[39] The sequence and antiamyloidogenic activity of the two hits are presented in Figure 2A. Both hits caused a dose-dependent reduction in A$\beta$ aggregation; however, cyclic D,L-$\alpha$-peptide [lLwHsK], **CP-1**, demonstrated somewhat better inhibitory activity in the low micromolar range and was therefore selected for further studies.

To elucidate the contribution of each amino acid to the total antiamyloidogenic activity of **CP-1**, an Ala scan study was performed. Here, each of the amino acids in **CP-1** was replaced, one at a time, with L-Ala or D-Ala according to the original amino acid configuration. The antiamyloidogenic activity of the analogues was then determined at 3 and 10 $\mu$M by the ThT assay. Table 1 summarizes the representative ThT results obtained from Ala-substituted derivatives of cyclic peptide **CP-1**.

Most of the Ala-substituted derivatives showed similar amyloid inhibitory activity at a 1:1 A$\beta$:peptide ratio. Nevertheless, Ala-mutated cyclic D,L-$\alpha$-peptides **w4a**, **L5A**, and **l6a** exhibited considerably lower antiamyloidogenic activity at a 1:1/3 A$\beta$:peptide ratio than the parent peptide ([lLwHsK], **CP-1**). Replacing Leu with the less hydrophobic Ala abolished antiamyloidogenic activity at a 1:1/3 ratio and considerably reduced activity at a 1:1 ratio in **L5A**. Similarly, antiamyloidogenic activity was reduced in **l6a** at a 1:1/3 ratio (but not at a 1:1 ratio). Substitution of D-Trp with D-Ala (to create **w4a**) completely arrested antiamyloidogenic activity at both of the tested ratios, which supports the importance of aromatic interactions in A$\beta$ binding and antiamyloidogenic activity.[40]

Because substituting Leu for Ala reduced the antiamyloidogenic effect of **L5A** and **I6a**, we tested the effect of more hydrophobic amino acids, such as norleucine (J in **L5J** or **CP-2**) and 2-aminooctanoic acid (Z in **L5Z**), on the antiamyloidogenic activity of **CP-1**. Replacing Leu with Z in **L5Z** had little effect on the antiamyloidogenic activity of the cyclic peptide, while J in **CP-2** preserved its activity as compared to that of **CP-1** (Table 1). **CP-2** also demonstrated potent antiamyloidogenic activity against A$\beta$42 (Figure S1), and therefore it was used for further studies.

Next, we determined the influence of intermolecular hydrogen bonding and cyclization on antiamyloidogenic activity. Previous studies have demonstrated that the antibacterial and antiviral activity of cyclic D,L-$\alpha$-peptides strongly correlate with the cyclic nature of the peptides and the intermolecular hydrogen-bond-directed self-assembly of the cyclic D,L-$\alpha$-peptide subunits.[29,30] Accordingly, a linear alternative D,L-$\alpha$-peptide and a linear all L-$\alpha$-peptide as well as a backbone *N*-methylated analogue of peptide **CP-2** were synthesized, and their activities were compared to that of the parent peptide, **CP-2**. In all cases, a significant decrease in inhibition was evident (Figure S2), suggesting that the cyclic nature of the peptides and intermolecular hydrogen bonding are crucial to their activity. Interestingly, many studies have shown that introducing backbone *N*-methyl groups onto peptides that bind A$\beta$ increases their antiamyloidogenic activity.[17,41] In contrast, our results suggest that intermolecular hydrogen bonding between A$\beta$ and the backbone of cyclic D,L-$\alpha$-peptides is essential for the binding of cyclic D,L-$\alpha$-peptides to A$\beta$ or, alternatively, that self-assembly of cyclic peptides is required for their activity.

The antiamyloidogenic activity of the selected analogues was also confirmed by transmission electron microscopy (TEM; Figure 2B,C and Figure S3). Samples that had been aged for 2 days were loaded onto TEM grids directly after the ThT experiments. As shown in Figure 2B, A$\beta$ tends to generate long unbranched fibrils as it ages. We found that coincubation of **CP-2** with soluble A$\beta$ drastically reduced fibril formation (Figure 2C). In control experiments, fibrils were still observed in the presence of the linear analogue, lJwHsK, and the *N*-methylated derivative [l(J)wH(s)K] (Figure S3). Notably, further TEM studies demonstrated that 2-day aged **CP-2** could also generate a fibrillar network (Figure S3), which is in accordance with previous studies suggesting that cyclic D,L-$\alpha$-peptides can self-assemble into peptide nanotubes.[27] Nevertheless, it seems that coincubation of **CP-2** with A$\beta$ resulted in the generation of coaggregates, which inhibited their mutual fibrillization. Our NMR analysis of fresh **CP-2** in PBS also revealed that it exists mainly in its self-assembled form (see below). Thus, these results, together with the low antiamyloidogenic activity of *N*-methylated **CP-2**, suggest that the bioactive form of **CP-2** is most likely aggregated or has a structure similar to that of the aggregated species.

To evaluate the effect of **CP-2** on the aggregation kinetics of A$\beta$, the ThT fluorescence of A$\beta$40 and A$\beta$42 was followed over


dx.doi.org/10.1021/ja310064v | *J. Am. Chem. Soc.* 2013, 135, 3474−3484

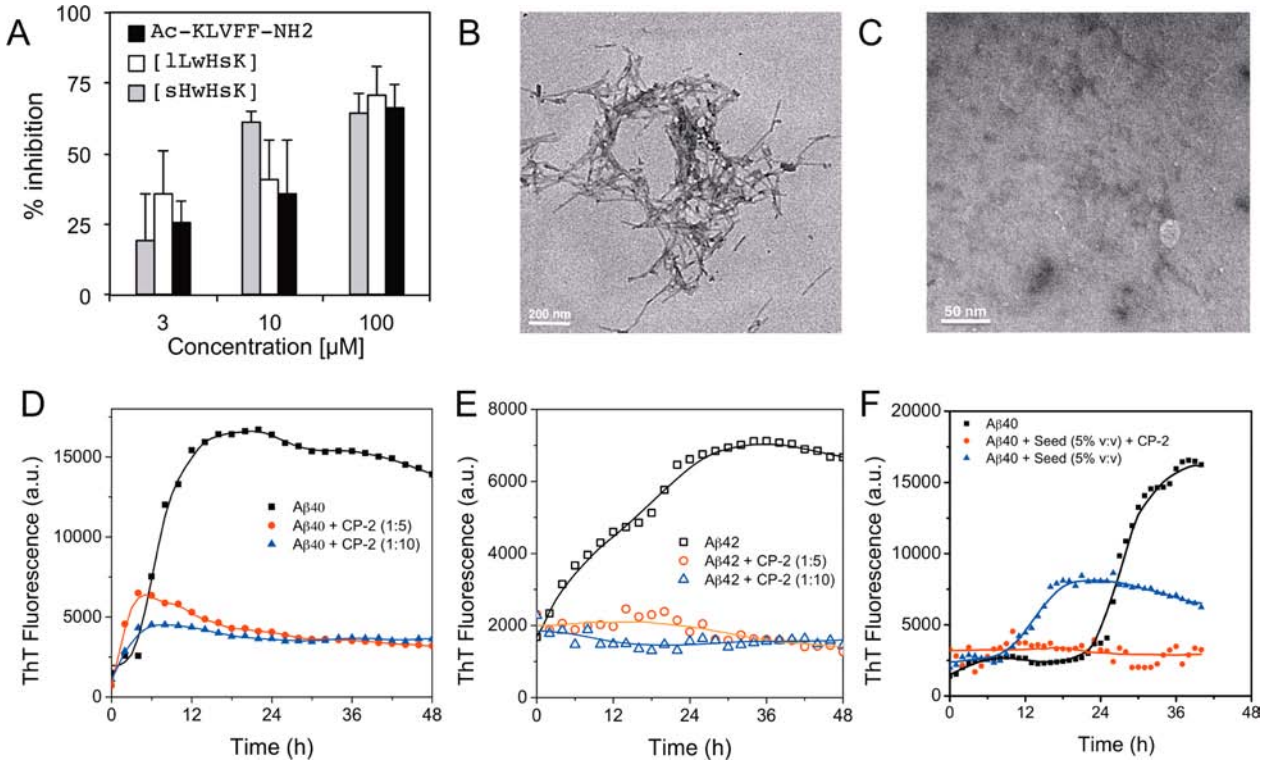


**Figure 2.** Antiamyloidogenic activity of cyclic D,L-$\alpha$-peptides discovered by library screening. (A) A$\beta$40 (10 $\mu$M) was incubated for 2 days at 37 °C in the presence or absence of the peptide analogues, and the degree of aggregation was determined using the ThT fluorescence assay. The ThT fluorescence value obtained from aged A$\beta$40 is referred to as 0% inhibition, while the value obtained from a PBS solution is referred to as 100% inhibition. The results are presented as the mean ± SD of three experiments ($n$ = 3). Single letter codes are used for amino acids (upper and lower case letters represent L- and D-amino acid residues, respectively). Square brackets are used to indicate a cyclic structure. TEM images of A$\beta$40 samples that were treated for 72 h (B) without or (C) with **CP-2** (100 $\mu$M). Negatively stained samples are shown. (D,E) ThT fluorescence kinetics of A$\beta$40 and A$\beta$42 in the presence or absence of **CP-2**. Monomeric (D) A$\beta$40 (10 $\mu$M) and (E) A$\beta$42 (20 $\mu$M) were incubated at 37 °C in a ThT solution (18 $\mu$M, 50 mM glycine in PBS, pH 7.4) in the absence or presence of 5- and 10-fold excesses of **CP-2** for 2 days under constant shaking, and the fluorescence was monitored over time. (F) Effect of **CP-2** (10-fold excess) on the kinetics of A$\beta$40 aggregation under seeding conditions. A$\beta$40 fibrils (100 $\mu$M; 5% v:v based on the amount of monomeric A$\beta$ and act as seeds) were sonicated for 5 min and incubated with either vehicle or **CP-2** (100 $\mu$M) for 5 min prior to the addition of monomeric A$\beta$40 (10 $\mu$M) solution containing ThT (18 $\mu$M). Fluorescence was then monitored up to 48 h. Experiments were carried out in triplicate and repeated twice.

**Table 1. Antiamyloidogenic Activity of the Cyclic D,L-$\alpha$-Peptide CP-1 and Its Ala-Substituted Analogues**

| | | inhibition of amyloidogenic activity (%)[b] | | |
|---|---|---|---|---|
| name | sequence[a] | 1:1 | 1:1/3 | retention time (min)[c] |
| **CP-1** | [lLwHsK] | 60 ± 7 | 32 ± 9 | 13.2 |
| **K1A** | [lLwHs**A**] | 67 ± 5 | 48 ± 6 | 14.2 |
| **s2a** | [lLwH**a**K] | 56 ± 4 | 39 ± 10 | 13.5 |
| **H3A** | [lLw**A**sK] | 69 ± 6 | 40 ± 8 | 14.4 |
| **w4a** | [lL**a**HsK] | 4 ± 4 | 5 ± 4 | 11.0 |
| **L5A** | [l**A**wHsK] | 44 ± 9 | 3 ± 10 | 11.0 |
| **l6a** | [**a**LwHsK] | 52 ± 12 | 12 ± 12 | 11.6 |
| **L5J (CP-2)** | [l**J**wHsK] | 69 ± 5 | 42 ± 10 | 13.5 |
| **L5Z** | [l**Z**wHsK] | 55 ± 14 | 30 ± 6 | 14.7 |

[a]Upper and lower case letters represent L- and D-amino acid residues, respectively. Square brackets indicate a cyclic structure. J and Z denote norleucine and 2-aminooctanoic acid, respectively. [b]Inhibition of amyloidogenic activity was determined by the ThT method using 10 $\mu$M of soluble A$\beta$40 at A$\beta$:CP-1 ratios of 1:1 and 1:1/3. See legend to Figure 2 for how antiamyloidogenic activity is derived form ThT fluorescence measurements. [c]Retention time on RP-C8.

2 days in the absence or presence of **CP-2** with constant shaking. In the absence of **CP-2**, the ThT fluorescence of A$\beta$40 (Figure 2D) gradually increased, after an initial lag time of 4 h, until it reached a plateau at ∼14 h, while the ThT fluorescence of A$\beta$42 increased immediately until reaching a plateau at 30 h (Figure 2E). The presence of **CP-2** dose-dependently decreased the aggregation of A$\beta$40, while it completely arrested the aggregation of A$\beta$42 even at a 1:5 A$\beta$:**CP-2** concentration ratio, which suggests that **CP-2** has a somewhat stronger inhibitory effect on the more neurotoxic A$\beta$42. The antiamyloidogenic activity of **CP-2** toward A$\beta$42 was also evident at a 1:1 A$\beta$:**CP-2** ratio (Figure S1).

To shed light on the mechanism of action of **CP-2**, we evaluated its effect on the kinetics of seed-induced A$\beta$ aggregation. Amyloid fibrils are seeding-competent structures that can efficiently convert soluble and monomeric proteins to their aggregated state.[42] Figure 2F shows that aggregation of monomeric A$\beta$40 is considerably accelerated in the presence of 5% A$\beta$40 seeds (v:v). Under the conditions we used for these studies, the lag time of A$\beta$ aggregation was shortened from ∼20 h for monomeric A$\beta$40 alone to ∼8 h when incubated in the presence of the seeds. We found that coincubation of **CP-2** with 5% A$\beta$ seeds and monomeric A$\beta$ completely inhibited the formation of A$\beta$ amyloids, suggesting that **CP-2** interacts either

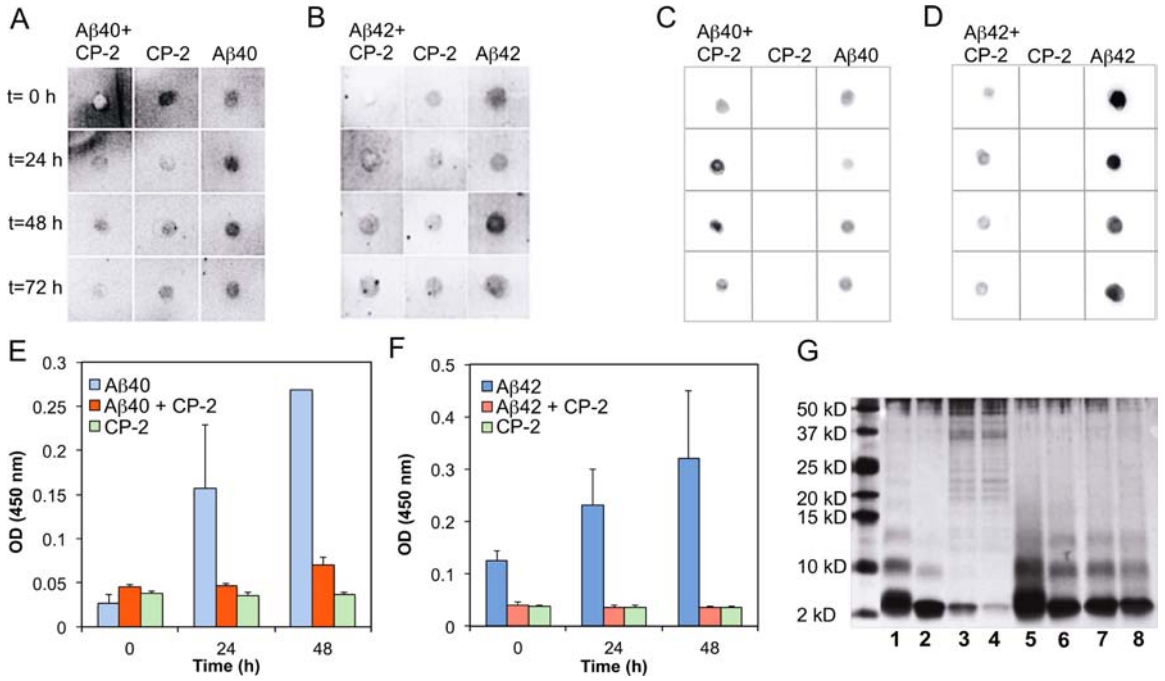


**Figure 3.** Effect of **CP-2**, [IJwHsK], on the remodeling of A$\beta$ conformation. (A) A$\beta$40 and (B) A$\beta$42 samples (50 $\mu$M) were aged for 0, 24, 48, or 72 h in the absence or presence of **CP-2** (500 $\mu$M), spotted onto nitrocellulose membranes, and probed with A11 antibody. (C,D) The same membranes were also immunostained with 6E10 antibody to confirm identical loading of the samples. Effect of **CP-2** on generation of (E) A$\beta$40- and (F) A$\beta$42-oligomers as tested by ELISA using the A$\beta$ oligomer-specific monoclonal antibody (OMAB). Experiments were carried out in triplicate and repeated twice. (G) Effect of **CP-2**, [IJwHsK], on oligomer distribution of A$\beta$40. A$\beta$40 samples (50 $\mu$M) were aged for 0, 24, 48, or 72 h in the absence (lanes 1−4) or presence (lanes 5−8) of **CP-2** (500 $\mu$M) and subjected to PICUP. Samples were then analyzed by SDS-PAGE and silver staining. The gel is representative of two experiments.

with the monomers and/or binds and remodels the seeds to incompetent structures, most likely via an "off-pathway" mechanism.[43]

Next, we tested whether **CP-2** can modulate the formation of soluble oligomers, which are considered the most toxic species in the A$\beta$ aggregation process.[15] Monomeric A$\beta$40 and A$\beta$42 were incubated with a 10-fold excess of **CP-2**, and oligomer formation was examined at various time intervals by dot blotting assay using the oligomer-specific polyclonal antibody A11, a conformational antibody that was originally raised against an oligomeric species of A$\beta$ and was found to react with toxic A$\beta$ as well as other unrelated protein oligomers.[15] Identical blots were also probed with the sequence-dependent 6E10 antibody to confirm the loading quality. In the absence of **CP-2**, the dot-blotting results showed a time-dependent increase in the amount of A11-reactive aggregates, which reached a maximum between 24 and 48 h of aggregation (Figure 3A,B). Co-incubation of A$\beta$40 (Figure 3A) or A$\beta$42 (Figure 3B) with **CP-2** reduced the intensity of A11-reactive species, particularly following 48−72 h of incubation. Remarkably, the nontoxic **CP-2** is also recognized by the A11 antibody (Figure 3A,B). This implies that **CP-2** and soluble A$\beta$ oligomers may have similar structural conformations, which could facilitate their cross-reaction. **CP-2** also reduced the reactivity of 6E10 toward A$\beta$42 (Figure 3D) and, to a lesser extent, toward A$\beta$40 (Figure 3C), suggesting that the interaction of **CP-2** with A$\beta$ impedes the ability of 6E10 to recognize A$\beta$.

The effect of **CP-2** on the A$\beta$ aggregation process was further followed by ELISA, using the A$\beta$ oligomer-specific monoclonal antibody (OMAB).[44] While aging of monomeric A$\beta$ gradually increased the amount of oligomeric species over a 48 h period (Figure 3E,F), as was observed using the A11 antibody (Figure 3A,B), the presence of **CP-2** dramatically reduced their amounts. Interestingly, the inhibitory effect of **CP-2** on oligomer aggregation was stronger for A$\beta$42 (Figure 3F) than for A$\beta$40 (Figure 3E). Further aging of A$\beta$ samples decreased the amount of OMAB-reactive oligomers (data not shown), most likely because of the generation of A$\beta$ fibrils that are not reactive toward the OMAB antibody. A decrease in antibody reactivity was also observed when A11 was incubated with 72 h-aged A$\beta$ (Figure 3A,B). These findings support our above seeding results that interaction of **CP-2** with A$\beta$ may alter the aggregation of A$\beta$ from an "on-pathway" to an "off-pathway" mechanism.[43]

We have also evaluated the effect of **CP-2** on A$\beta$ oligomer distribution. Studies have shown that LMW oligomeric intermediates of A$\beta$ are potent neurotoxins. In particular, dodecameric oligomer assemblies (~56 kDa) of A$\beta$42 and A$\beta$ intermediates that are recognized by the conformation-specific A11 antibody have been suggested to be the key effectors of neurotoxicity in AD.[15,45−47] Because the A$\beta$ oligomers exist under conditions of dynamic equilibrium, the PICUP method was used to stabilize these species and determine their oligomerization state by SDS/PAGE.[35] The distribution of PICUP-derived oligomers of A$\beta$40 revealed the presence of several oligomeric species whose lengths ranged from monomer to pentamer, with monomers as the most abundant species (Figure 3G, lane 1). Following the aging process, a time-dependent decrease in the amounts of A$\beta$ monomers and small oligomers (2−5-mers) was evident, which was concomitant with the appearance of LMW A$\beta$ (Figure 3G, lanes 3, 4). More specifically, LMW species were observed after 48 h of aging (Figure 3G, lane 3), when according to dot blot and ELISA


dx.doi.org/10.1021/ja310064v | J. Am. Chem. Soc. 2013, 135, 3474−3484

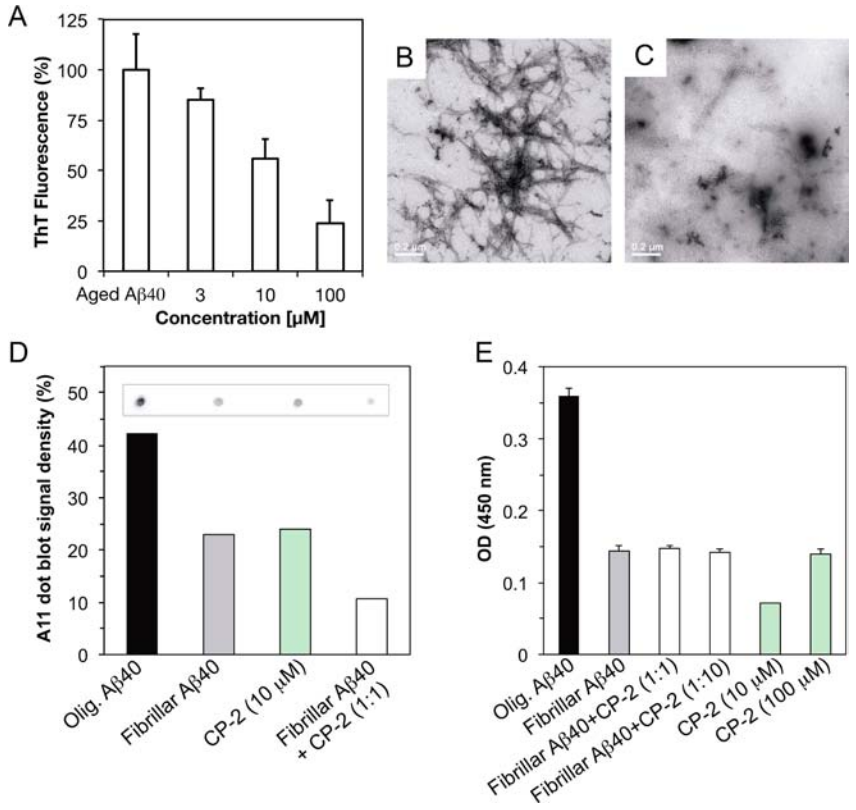


**Figure 4. CP-2**, [lJwHsK], disassembles fibrillar A$\beta$40 to species that are not reactive toward A11- and OMAB-antibodies. (A) A$\beta$40 (10 $\mu$M) was aged for 4 days to afford maximal ThT fluorescence. The aged samples were then incubated with freshly prepared cyclic peptide **CP-2** (3, 10, or 100 $\mu$M) for a further 72 h and then examined by the ThT assay. The ThT fluorescence values (~10 000 au) of aged A$\beta$40 represent 100% ThT fluorescence, while those of PBS alone (~2000 au) represent 0% ThT fluorescence. Results are the mean ± SD from 3 to 5 assays ($n$ = 3 each). The disaggregation of (B) A$\beta$ fibrils to (C) amorphous aggregates was examined using TEM. The disaggregation products of A$\beta$ fibrils were also tested by (D) dot blotting assay using the A11 antibody and (E) ELISA using the OMAB antibody to detect the possible generation of neurotoxic amyloid oligomers. A$\beta$40 oligomers were generated by aging monomeric A$\beta$40 for 48 h.

experiments the concentration of soluble aggregates increases dramatically (Figure 3). The addition of **CP-2** to A$\beta$ solution dramatically reduced the amount of LMW A$\beta$ (Figure 3G, lanes 7 and 8 (with **CP-2**) vs lanes 3 and 4 (without **CP-2**)) and stabilized the 1−3-mers (Figure 3G, lanes 6−8). These results suggest that **CP-2** is capable of binding early A$\beta$ oligomers, which may lead to the disaggregation of A$\beta$ aggregates and fibrils by shifting the equilibrium toward short oligomers.

To examine whether cyclic D,L-$\alpha$-peptide **CP-2** can disassemble aggregated or fibrillar A$\beta$, A$\beta$40 was aged for 4 days at 37 °C to form aggregates/fibrils and then exposed to increasing concentrations of **CP-2** for a further 72 h. Although aged A$\beta$ exhibited a pronounced ThT signal, the addition of fresh cyclic peptide **CP-2** reduced the signal in a dose-dependent manner (Figure 4A). The near-stoichiometric excess of **CP-2** required for effective disassembly most likely suggests that the active **CP-2** conformation generates relatively stable 1:1 coaggregates with monomeric or small oligomers (1−3 mers) of A$\beta$, and shifts the aggregation equilibrium toward these species, provided that the overall concentrations are high enough to allow assembly of these coaggregates. The disaggregation of fibrillar A$\beta$ by **CP-2** was also confirmed by TEM analysis (Figure 4B,C), which showed the transformation of the fibrillar network (Figure 4B) to amorphous-like structures (Figure 4C).

The disassembly of A$\beta$ fibrils by **CP-2** could conceivably produce adverse effects in vivo if it increases the amount of toxic intermediates.[6,48,49] To confirm that the disaggregation of A$\beta$ fibrils does not involve the formation of toxic soluble oligomers, **CP-2**-treated A$\beta$ fibrils were tested for their reactivity toward the A11 (Figure 4D) and OMAB antibodies (Figure 4E). Soluble A$\beta$ oligomers generated from monomeric A$\beta$40 that had been aged for 48 h were used as the control. The results suggest that disaggregation of the A$\beta$ fibrils by a near-stoichiometric concentration of **CP-2** leads to the generation of coaggregates that are distinct from soluble aggregates (Figure 4D,E).

Because self-assembly and aggregation of A$\beta$ are associated with pathogenesis in AD, we next probed whether **CP-2** could reduce A$\beta$-induced toxicity in rat pheochromocytoma PC12 cells. Cells were incubated for 24 h with A$\beta$40 (10 $\mu$M) or A$\beta$42 (20 $\mu$M) that had been aged for 48 h with increasing concentrations of cyclic D,L-$\alpha$-peptide **CP-2**. Cell viability was then assessed by the MTT assay. Figure 5 shows that cyclic peptide **CP-2** dose-dependently decreased A$\beta$-induced toxicity to PC12 cells. A maximal increase in cell viability was observed when A$\beta$ was incubated with a 5−10-fold excess of the cyclic peptide. Interestingly, incubation of A$\beta$40 with the *N*-methylated analogue of **CP-2**, [l(J)wH(s)K], which showed lower antiamyloidogenic activity in the ThT assay, had a minimal effect on toxicity, thereby further confirming the importance of backbone hydrogens in antiamyloidogenic activity. In control experiments, cyclic peptide **CP-2** was found to be nontoxic to PC12 cells even at the highest tested


dx.doi.org/10.1021/ja310064v | J. Am. Chem. Soc. 2013, 135, 3474−3484

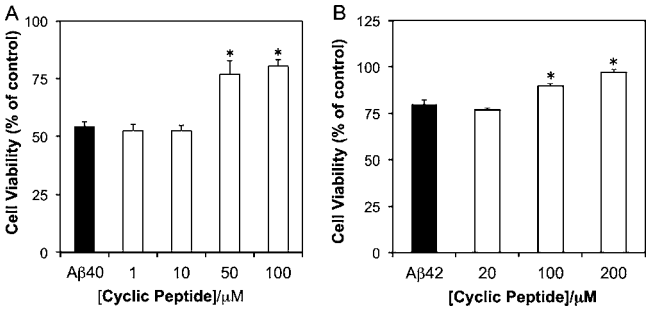


**Figure 5.** Dose-dependent effect of **CP-2** on A$\beta$-mediated toxicity to PC12 cells. (A) A$\beta$40 (10 $\mu$M) or (B) A$\beta$42 (20 $\mu$M) was aged in the absence or presence of increasing concentrations of **CP-2** for 48 h and then exposed to PC12 cells for a further 24 h. Cell viability was then determined by the MTT assay. Results are expressed as a percentage of the control (untreated) cells and are reported as mean ± SD from three assays ($n$ = 4–6 each). Significance (*, $p < 0.05$) was calculated relative to A$\beta$40 (10 $\mu$M) or A$\beta$42 (20 $\mu$M), respectively.

concentration (200 $\mu$M). Assuming that A$\beta$ is present in the brain at subnanomolar concentrations,[50] it remains to be seen whether **CP-2** will be effective in reducing the A$\beta$ burden, in vivo.

To acquire more detailed knowledge of the mechanism by which **CP-2** interacts with soluble or aggregated A$\beta$, far UV-circular dichroism (far-UV CD) spectroscopy studies were carried out (Figure 6). These experiments focused on the effect

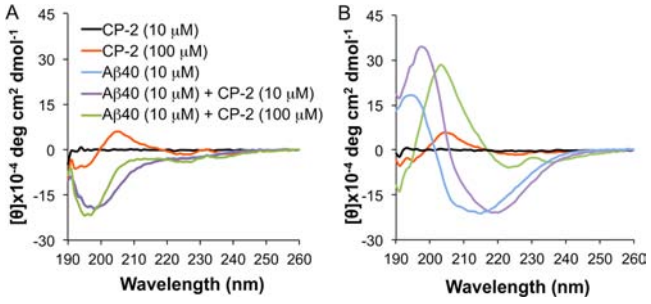


**Figure 6.** Effect of **CP-2**, [lJwHsK], on the structural transition of A$\beta$ from a random coil to $\beta$-sheet structure. Time dependent far-UV CD spectra of freshly prepared A$\beta$40 monomer (10 $\mu$M) incubated in the absence or presence of **CP-2** (10 and 100 $\mu$M) in phosphate buffer (50 mM, pH 7.4) and analyzed after 0 h (A) and 24 h (B). The spectra of **CP-2** alone at the same concentrations are also shown. Data are representative of two independent experiments.

of **CP-2** on structural transitions that occur early in the A$\beta$ aggregation process. In the absence of **CP-2**, A$\beta$ undergoes secondary structural changes over time from a random coil characterized by a negative CD peak around 197 nm (Figure 6A; the blue line (which is largely overlain by the purple line)) to a $\beta$-sheet-rich structure with a positive band around 195 nm and a negative band at 215 nm (Figure 6B).[51] Co-incubation of A$\beta$ with **CP-2** (10 $\mu$M) for 24 h caused a small shift of the spectrum to higher wavelengths (positive and negative peaks at 197 and 218 nm, respectively). The shift of the negative minimum toward higher wavelengths could suggest a reduction in antiparallel $\beta$-sheet content and an increase in parallel $\beta$-sheet content.[52] On the other hand, incubation of a higher concentration of **CP-2** (100 $\mu$M) with A$\beta$ completely changed the CD spectrum after 24 h to what appears to be an aggregated $\beta$-sheet with a strong positive band at 203 nm and a negative band at 223 nm (Figure 6B, green line).[52] The shifting of the minimum to 223 nm could again suggest formation of a parallel $\beta$-sheet. The negative band at 235 nm seen in the spectrum of **CP-2** alone or with A$\beta$40 (100 $\mu$M; Figure 6) implies probable Trp–Trp interactions generated from the self-assembly of **CP-2** into peptide nanotubes.[53] This band is missing in the CD spectrum of the *N*-methylated analogue (Figure S4), which is unable to self-assemble because of steric hindrance from the *N*-methyl groups. The CD bands associated with a parallel $\beta$-structure are seen also in the weak CD spectrum of **CP-2** alone (100 $\mu$M), which is in agreement with previous studies suggesting that cyclic D,L-$\alpha$-peptides can adopt either a parallel or an antiparallel $\beta$-sheet conformation depending on the physicochemical properties of the side chains.[27,54] Overall, our CD observations suggest that the incubation of A$\beta$ with a 10-fold greater concentration of **CP-2** transforms the conformation of the whole sample toward $\beta$-structures, most likely with dominant parallel $\beta$-structure. In contrast, incubation of A$\beta$ with an equimolar concentration of the *N*-methylated derivative of **CP-2** ([l(J)wH(s)K]; 10 $\mu$M) had no significant effect on the antiparallel structure of A$\beta$ (positive band around 195 nm and a negative band at 217 nm, Figure S4). Incubation of A$\beta$ with a higher concentration of [l(J)wH(s)K] (100 $\mu$M) generated a CD signal with a positive peak at around 196 nm and a negative signal at around 228 nm (Figure S4; orange line). An identical CD signature structure is seen also in the weak spectrum of 100 $\mu$M [l(J)wH(s)K] (Figure S4, pink line). Interestingly, very recent studies have suggested that the toxic oligomeric form of A$\beta$ may preferentially adopt antiparallel conformations,[5,55–57] whereas the fibrils formed later in the aggregation process and investigated by solid-state NMR show parallel $\beta$-structures.[26] Thus, our CD and toxicity results are in agreement with these observations, and selective targeting of the putatively more toxic antiparallel conformations may have important implications for the development of new therapeutics.

To obtain more detailed information about molecular interactions between A$\beta$40 and **CP-2**, NMR studies were performed. The NMR spectrum of **CP-2** in 1:1 $D_2O$:DMSO-$d_6$ consists of well-resolved NMR signals (Figure S5). Line-broadening causes these signals to disappear almost entirely in phosphate buffer, suggesting that the cyclic peptide quickly self-assembles into a larger aggregated state in a water-based environment. NMR diffusion measurements confirmed that **CP-2** is monomeric, or possibly arranged in very small assemblies, when dissolved in 50–100% DMSO (data not shown), as would be expected from the well-behaved NMR signals (Figure S5). Interestingly, the critical micelle concentration (cmc) of **CP-2** alone (48 $\mu$M) in aqueous PBS solution also confirmed that the peptide forms aggregates at the concentration used for NMR studies, while the *N*-methylated derivative, [l(J)wH(s)K], self-assembled at a higher concentration (102 $\mu$M; Figure S6D), as expected.

Figure 7 shows the amide region of the $^1H-^{15}N$ HSQC NMR spectra at +5 °C obtained from titrating increasing concentrations of **CP-2** against A$\beta$40. At the beginning of the titration, the NMR spectrum of the A$\beta$ peptide in its monomeric form derives from an essentially random coil structure with some influence of a left-handed $3_1$ helix.[58] Addition of **CP-2** to A$\beta$40 induces concentration-dependent chemical shift changes, confirming a fast (on the NMR time scale) interaction between the two molecules (Figure 7 and Figure S7). Chemical shift changes in the backbone amide


dx.doi.org/10.1021/ja310064v | J. Am. Chem. Soc. 2013, 135, 3474–3484

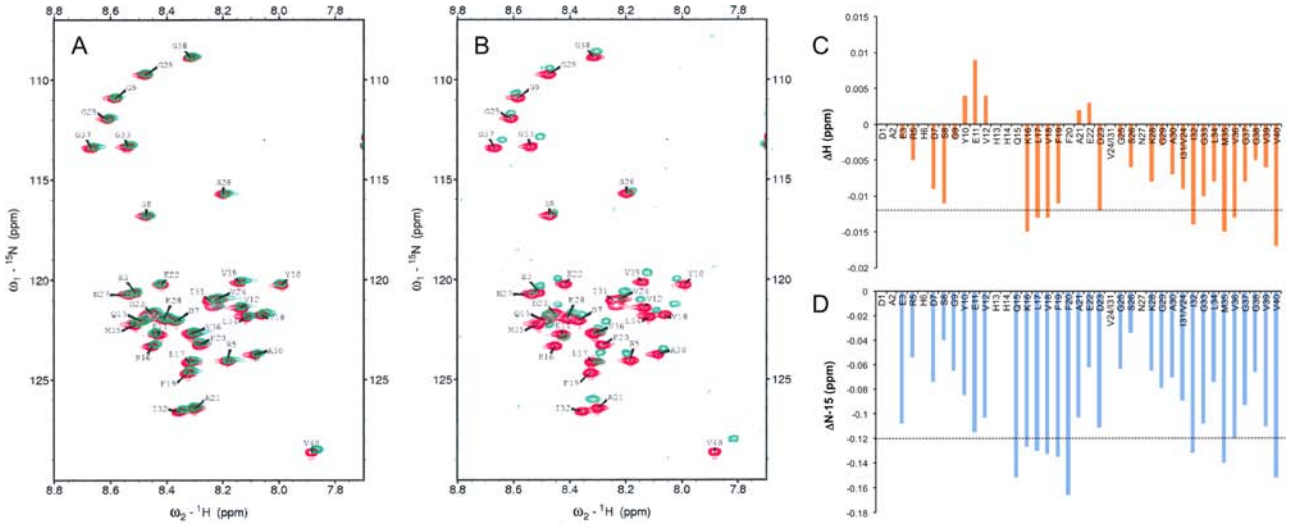


**Figure 7.** $^1$H−$^{15}$N HSQC spectra of 75 $\mu$M $^{15}$N-A$\beta$40 peptide alone (red peaks) and after the addition of cyclic D,L-$\alpha$-peptide **CP-2** at a concentration of either (A) 375 $\mu$M (green peaks, 1:5 ratio) or (B) 1875 $\mu$M (green peaks, 1:25 ratio). NMR chemical shift changes for (C) $^1$H and (D) $^{15}$N resonances of 50 $\mu$M $^{15}$N-A$\beta$40, induced by 100 $\mu$M **CP-2** and corrected for the chemical shifts induced by 1 M DMSO-$d_6$. The data were obtained from $^1$H−$^{15}$N-HSQC experiments run at +5 °C in 10 mM phosphate buffer, pH 7.4.

groups of A$\beta$40 induced by **CP-2** and corrected for the slight DMSO effect are presented in Figure 7C,D. Although the changes are small relative to those expected for a full transition to $\alpha$-helix or $\beta$-sheet, there is a residue pattern resembling those reported in previous studies of A$\beta$40 in various environments. The largest chemical shift effects are seen for residues 16−23, 31−37, and the C-terminus (Figure 7B). The sign of the changes in both the $^1$H and the $^{15}$N dimensions suggests weak induction of $\alpha$-helix structure in the peptide. Previous observations of the A$\beta$ peptide have shown $\alpha$-helix induction from interaction with sodium dodecyl sulfate micelles,[59] or induction of $\beta$-hairpin conformation when interacting with selected affibody proteins.[60,61] In both cases, hydrogen bonding within the 17−23 and 30−36 regions was evident. These regions are also involved in the formation of parallel $\beta$-strands in A$\beta$42 fibrils.[26] We conclude that these A$\beta$ segments are prone to engage in H-bonding, either within the cyclic peptide monomer or with their complementary A$\beta$ strands, depending on the environment. Mounting evidence, including the observations shown in the present study, suggests that the A$\beta$ peptide may probe different secondary structures in a kinetic aggregation process, which may involve transitions from one secondary structure to the next until a stable state is reached in the form of large and ordered fibrils. In the present study, the induced structural changes may be toward an $\alpha$-helix conformation (on the basis of the NMR evidence for monomeric peptide) during the initial stage of aggregation in the presence of **CP-2**, followed by a shift to a parallel $\beta$-structure (on the basis of the CD evidence from the aggregating peptide) after aging of the A$\beta$−**CP-2** coaggregates.

We also found that excess addition of **CP-2** to A$\beta$40 caused a gradual disappearance of the A$\beta$ NMR signal, most probably because of coaggregation and/or chemical exchange between various conformations of the A$\beta$ peptide occurring on an intermediate time scale. A similar loss of A$\beta$40 NMR signal has been observed previously upon titration of A$\beta$ with sodium dodecyl sulfate, while parallel CD studies showed distinct evidence for $\beta$-structure induction.[36] Recent studies of similar NMR-invisible coaggregates of A$\beta$40 with the small organic molecules Congo red and lacmoid have revealed that it is possible to characterize the kinetics of the molecular interactions by observing NMR relaxation dispersion effects on the remaining monomeric A$\beta$40 NMR signals.[62] A similarity between the Congo red/lacmoid systems and the present cyclic D,L-$\alpha$-peptide architecture of **CP-2** is that they both display supramolecular structures in aqueous solution by themselves.[63] The Congo red/lacmoid assemblies appear to be in dynamic exchange with A$\beta$ monomers, forming slowly growing coaggregates that redirect A$\beta$ away from the self-assembly pathways associated with cellular toxicity. A similar process may also be relevant for **CP-2**.

The interaction between A$\beta$40 and **CP-2** was also monitored by 1D NMR titrations (Figure S7). Clear chemical shift changes are observed in the aromatic region of A$\beta$40 even at low concentrations of **CP-2**. This corroborates our ThT results regarding the importance of the aromatic interaction (via Trp) in antiamyloidogenic activity. In the samples with a high concentration of **CP-2**, we could also detect new NMR signals in the 3−4 ppm region (Figure S7), appearing at ppm values associated with neither A$\beta$40 nor the cyclic peptide alone. Hence, the new signals appear to originate from an A$\beta$40−cyclic peptide complex. Some of these new signals are relatively sharp, indicating that the complex formed is not overly large (in NMR terms), and future analysis and possible assignment of these new signals may provide more information on the details of the specific interaction between A$\beta$40 and the cyclic peptide.

Taken together, the above spectroscopic results provide evidence for interactions between monomeric and low oligomeric A$\beta$40 and **CP-2**, where the latter most likely appears in a self-assembled form, and the former possibly adopts a monomeric $\alpha$-helix form upon its first interaction with **CP-2**.

## ■ CONCLUSIONS

Many pathological protein amyloids exhibit similar structural and functional properties that are responsible for their direct toxicity to cells. The self-assembled cyclic D,L-$\alpha$-peptides display many of the chemical and biochemical properties of the amyloids and, as revealed in this study, can cross-interact with

Aβ and modulate its aggregation and toxicity. Here, we showed that this class of abiotic architecture interacts with small oligomeric form of Aβ (1−3 mer) and may stabilize a parallel β-sheet conformation. Presently, there is intense debate about the structural properties and biological effects of transient oligomeric intermediates involved in the process of amyloid formation, particularly regarding Aβ, but also in connection with other amyloidogenic proteins, such as α-synuclein (reviewed in ref 5). Several lines of evidence link the oligomeric states of the amyloidogenic proteins, rather than their final and stable fibrillar states, with their potent toxicity.[6,7,13,15,45] Although structural heterogeneity abounds in amyloidogenic proteins, solid-state NMR, FT-IR, and X-ray crystallography studies of selected proteins suggest that early oligomeric states may be composed of antiparallel β structures, which may be transformed at later stages to parallel β structures.[55−57] For Aβ, the antiparallel β structures would then be the most active neurotoxic agents, and avoiding their accumulation by redirecting the aggregation pathway could be an efficient way to decrease Aβ's cytotoxicity.

This hypothesis is strengthened by the present results on the effects of the cyclic peptide **CP-2** on Aβ aggregation and toxicity. Some important effects of the cyclic D,L-α-peptide **CP-2** on Aβ aggregation and conformation can be summarized as follows. (a) The ThT fluorescence intensity of Aβ40/42−**CP-2** mixtures decreases over time, suggesting the presence of less amyloidogenic material at later time periods (Table 1). (b) **CP-2** drastically decreases the effect of Aβ seeds. (c) TEM studies show that **CP-2** affects the final structures of Aβ aggregates such that, according to dot blotting and ELISA experiments, they contain smaller amounts of the toxic conformation(s) (Figures 2 and 3). (d) The cell toxicity of aged Aβ is reduced by the presence of **CP-2** (Figure 5). (e) The size distribution of Aβ oligomers is shifted toward smaller sizes in the presence of **CP-2** (Figure 3G). (f) The structural transition that occurs during the aggregation of Aβ in the absence compared with the presence of **CP-2** suggests that **CP-2** may promote the conformational transition of Aβ aggregates from an antiparallel β-sheet conformation toward parallel β structures (Figure 6). On the basis of these observations, we hypothesize that the effects of cyclic peptide **CP-2** arise from shifting the Aβ aggregation pathway to an "off-pathway" mechanism that yields relatively short oligomeric or amorphous assemblies that contain a large fraction of less cytotoxic parallel β-sheet structures. Further studies will show if this kind of change in the aggregation chemistry is also beneficial for lowering the amount of toxic oligomers in the brains of transgenic animals and alleviating the symptoms associated with AD.

## ■ ASSOCIATED CONTENT

### Ⓢ Supporting Information

Full experimental details, Scheme S1, Figures S1−7, and related references. This material is available free of charge via the Internet at http://pubs.acs.org.

## ■ AUTHOR INFORMATION


### Corresponding Author

rahimis@biu.ac.il

### Author Contributions

§These authors contributed equally.


### Notes

The authors declare no competing financial interest.

## ■ ACKNOWLEDGMENTS

This work was supported in part by a grant from the Chief Scientist of the Israel Ministry of Health and Israel Ministry for Senior Citizens (to S.R.) and grants from the Swedish Research Council and the Knut and Alice Wallenberg Foundation (to A.G.).

## ■ REFERENCES


(1) Chiti, F.; Dobson, C. M. *Annu. Rev. Biochem.* **2006**, *75*, 333.
(2) Stefani, M.; Dobson, C. M. *J. Mol. Med.* **2003**, *81*, 678.
(3) Hardy, J.; Selkoe, D. J. *Science* **2002**, *297*, 353.
(4) Lansbury, P. T.; Lashuel, H. A. *Nature* **2006**, *443*, 774.
(5) Fändrich, M. *J. Mol. Biol.* **2012**, *421*, 427.
(6) Haass, C.; Selkoe, D. J. *Nat. Rev. Mol. Cell Biol.* **2007**, *8*, 101.
(7) Lambert, M. P.; Barlow, A. K.; Chromy, B. A.; Edwards, C.; Freed, R.; Liosatos, M.; Morgan, T. E.; Rozovsky, I.; Trommer, B.; Viola, K. L.; Wals, P.; Zhang, C.; Finch, C. E.; Krafft, G. A.; Klein, W. L. *Proc. Natl. Acad. Sci. U.S.A.* **1998**, *95*, 6448.
(8) Schenk, D.; Barbour, R.; Dunn, W.; Gordon, G.; Grajeda, H.; Guido, T.; Hu, K.; Huang, J.; Johnson-Wood, K.; Khan, K.; Kholodenko, D.; Lee, M.; Liao, Z.; Lieberburg, I.; Motter, R.; Mutter, L.; Soriano, F.; Shopp, G.; Vasquez, N.; Vandevert, C.; Walker, S.; Wogulis, M.; Yednock, T.; Games, D.; Seubert, P. *Nature* **1999**, *400*, 173.
(9) DeMattos, R. B.; Bales, K. R.; Cummins, D. J.; Dodart, J. C.; Paul, S. M.; Holtzman, D. M. *Proc. Natl. Acad. Sci. U.S.A.* **2001**, *98*, 8850.
(10) Frydman-Marom, A.; Rechter, M.; Shefler, I.; Bram, Y.; Shalev, D. E.; Gazit, E. *Angew. Chem., Int. Ed.* **2009**, *48*, 1981.
(11) Hochdörffer, K.; März-Berberich, J.; Nagel-Steger, L.; Epple, M.; Meyer-Zaika, W.; Horn, A. H.; Sticht, H.; Sinha, S.; Bitan, G.; Schrader, T. *J. Am. Chem. Soc.* **2011**, *133*, 4348.
(12) Härd, T.; Lendel, C. *J. Mol. Biol.* **2012**, *421*, 441.
(13) Kirkitadze, M. D.; Condron, M. M.; Teplow, D. B. *J. Mol. Biol.* **2001**, *312*, 1103.
(14) Anderson, V. L.; Ramlall, T. F.; Rospigliosi, C. C.; Webb, W. W.; Eliezer, D. *Proc. Natl. Acad. Sci. U.S.A.* **2010**, *107*, 18850.
(15) Kayed, R.; Head, E.; Thompson, J. L.; McIntire, T. M.; Milton, S. C.; Cotman, C. W.; Glabe, C. G. *Science* **2003**, *300*, 486.
(16) Rebek, J., Jr. *Proc. Natl. Acad. Sci. U.S.A.* **2009**, *106*, 10423.
(17) Yan, L. M.; Velkova, A.; Tatarek-Nossol, M.; Andreetto, E.; Kapurniotu, A. *Angew. Chem., Int. Ed.* **2007**, *46*, 1246.
(18) Mandal, P. K.; Pettegrew, J. W.; Masliah, E.; Hamilton, R. L.; Mandal, R. *Neurochem. Res.* **2006**, *31*, 1153.
(19) Buxbaum, J. N.; Ye, Z.; Reixach, N.; Friske, L.; Levy, C.; Das, P.; Golde, T.; Masliah, E.; Roberts, A. R.; Bartfai, T. *Proc. Natl. Acad. Sci. U.S.A.* **2008**, *105*, 2681.
(20) Rank, K. B.; Pauley, A. M.; Bhattacharya, K.; Wang, Z.; Evans, D. B.; Fleck, T. J.; Johnston, J. A.; Sharma, S. K. *FEBS Lett.* **2002**, *514*, 263.
(21) Velkova, A.; Tatarek-Nossol, M.; Andreetto, E.; Kapurniotu, A. *Angew. Chem., Int. Ed.* **2008**, *47*, 7114.
(22) Nicolls, M. R. *Curr. Alzheimer Res.* **2004**, *1*, 47.
(23) Seeliger, J.; Evers, F.; Jeworrek, C.; Kapoor, S.; Weise, K.; Andreetto, E.; Tolan, M.; Kapurniotu, A.; Winter, R. *Angew. Chem., Int. Ed.* **2012**, *51*, 679.
(24) Quist, A.; Doudevski, I.; Lin, H.; Azimova, R.; Ng, D.; Frangione, B.; Kagan, B.; Ghiso, J.; Lal, R. *Proc. Natl. Acad. Sci. U.S.A.* **2005**, *102*, 10427.
(25) Shai, Y.; Bach, D.; Yanovsky, A. *J. Biol. Chem.* **1990**, *265*, 20202.
(26) Lührs, T.; Ritter, C.; Adrian, M.; Riek-Loher, D.; Bohrmann, B.; Dobeli, H.; Schubert, D.; Riek, R. *Proc. Natl. Acad. Sci. U.S.A.* **2005**, *102*, 17342.
(27) Ghadiri, M. R.; Granja, J. R.; Milligan, R. A.; McRee, D. E.; Khazanovich, N. *Nature* **1993**, *366*, 324.
(28) Sanchez-Quesada, J.; Isler, M. P.; Ghadiri, M. R. *J. Am. Chem. Soc.* **2002**, *124*, 10004.

(29) Fernandez-Lopez, S.; Kim, H. S.; Choi, E. C.; Delgado, M.; Granja, J. R.; Khasanov, A.; Kraehenbuehl, K.; Long, G.; Weinberger, D. A.; Wilcoxen, K. M.; Ghadiri, M. R. *Nature* **2001**, *412*, 452.
(30) Montero, A.; Gastaminza, P.; Law, M.; Cheng, G.; Chisari, F. V.; Ghadiri, M. R. *Chem. Biol.* **2011**, *18*, 1453.
(31) Lam, K. S.; Salmon, S. E.; Hersh, E. M.; Hruby, V. J.; Kazmierski, W. M.; Knapp, R. J. *Nature* **1991**, *354*, 82.
(32) Liu, R. W.; Mark, J.; Lam, K. S. *J. Am. Chem. Soc.* **2002**, *124*, 7678.
(33) Zagorski, M. G.; Yang, J.; Shao, H.; Ma, K.; Zeng, H.; Hong, A. *Methods Enzymol.* **1999**, *309*, 189.
(34) Richman, M.; Wilk, S.; Skirtenko, N.; Perelman, A.; Rahimipour, S. *Chem.-Eur. J.* **2011**, *17*, 11171.
(35) Bitan, G.; Lomakin, A.; Teplow, D. B. *J. Biol. Chem.* **2001**, *276*, 35176.
(36) Wahlström, A.; Hugonin, L.; Peralvarez-Marin, A.; Jarvet, J.; Gräslund, A. *FEBS J.* **2008**, *275*, 5117.
(37) LeVine, H., III. *Protein Sci.* **1993**, *2*, 404.
(38) Redman, J. E.; Wilcoxen, K. M.; Ghadiri, M. R. *J. Comb. Chem.* **2003**, *5*, 33.
(39) Tjernberg, L. O.; Naslund, J.; Lindqvist, F.; Johansson, J.; Karlstrom, A. R.; Thyberg, J.; Terenius, L.; Nordstedt, C. *J. Biol. Chem.* **1996**, *271*, 8545.
(40) Gazit, E. *FASEB J.* **2002**, *16*, 77.
(41) Gordon, D. J.; Tappe, R.; Meredith, S. C. *J. Pept. Res.* **2002**, *60*, 37.
(42) Harper, J. D.; Lansbury, P. T., Jr. *Annu. Rev. Biochem.* **1997**, *66*, 385.
(43) Ehrnhoefer, D. E.; Bieschke, J.; Boeddrich, A.; Herbst, M.; Masino, L.; Lurz, R.; Engemann, S.; Pastore, A.; Wanker, E. E. *Nat. Struct. Mol. Biol.* **2008**, *15*, 558.
(44) Lindhagen-Persson, M.; Brannstrom, K.; Vestling, M.; Steinitz, M.; Olofsson, A. *PLoS One* **2010**, *5*, e13928.
(45) Walsh, D. M.; Klyubin, I.; Fadeeva, J. V.; Cullen, W. K.; Anwyl, R.; Wolfe, M. S.; Rowan, M. J.; Selkoe, D. J. *Nature* **2002**, *416*, 535.
(46) Bernstein, S. L.; Dupuis, N. F.; Lazo, N. D.; Wyttenbach, T.; Condron, M. M.; Bitan, G.; Teplow, D. B.; Shea, J. E.; Ruotolo, B. T.; Robinson, C. V.; Bowers, M. T. *Nat. Chem.* **2009**, *1*, 326.
(47) Lesne, S.; Koh, M. T.; Kotilinek, L.; Kayed, R.; Glabe, C. G.; Yang, A.; Gallagher, M.; Ashe, K. H. *Nature* **2006**, *440*, 352.
(48) Carulla, N.; Caddy, G. L.; Hall, D. R.; Zurdo, J.; Gairi, M.; Feliz, M.; Giralt, E.; Robinson, C. V.; Dobson, C. M. *Nature* **2005**, *436*, 554.
(49) Martins, I. C.; Kuperstein, I.; Wilkinson, H.; Maes, E.; Vanbrabant, M.; Jonckheere, W.; Van Gelder, P.; Hartmann, D.; D'Hooge, R.; De Strooper, B.; Schymkowitz, J.; Rousseau, F. *EMBO J.* **2008**, *27*, 224.
(50) Sengupta, P.; Garai, K.; Sahoo, B.; Shi, Y.; Callaway, D. J.; Maiti, S. *Biochemistry* **2003**, *42*, 10506.
(51) Tilstra, L.; Mattice, W. L. In *Circular Dichroism and the Conformational Analysis of Biomolecules*; Fasman, G. D., Ed.; Plenum Press: New York, 1996, p ix.
(52) Balcerski, J. S.; Pysh, E. S.; Bonora, G. M.; Toniolo, C. *J. Am. Chem. Soc.* **1976**, *98*, 3470.
(53) Ajikumar, P. K.; Lakshminarayanan, R.; Ong, B. T.; Valiyaveettil, S.; Kini, R. M. *Biomacromolecules* **2003**, *4*, 1321.
(54) Kobayashi, K.; Granja, J. R.; Ghadiri, M. R. *Angew. Chem., Int. Ed. Engl.* **1995**, *34*, 95.
(55) Cerf, E.; Sarroukh, R.; Tamamizu-Kato, S.; Breydo, L.; Derclaye, S.; Dufrene, Y. F.; Narayanaswami, V.; Goormaghtigh, E.; Ruysschaert, J. M.; Raussens, V. *Biochem. J.* **2009**, *421*, 415.
(56) Qiang, W.; Yau, W. M.; Luo, Y.; Mattson, M. P.; Tycko, R. *Proc. Natl. Acad. Sci. U.S.A.* **2012**, *109*, 4443.
(57) Laganowsky, A.; Liu, C.; Sawaya, M. R.; Whitelegge, J. P.; Park, J.; Zhao, M.; Pensalfini, A.; Soriaga, A. B.; Landau, M.; Teng, P. K.; Cascio, D.; Glabe, C.; Eisenberg, D. *Science* **2012**, *335*, 1228.
(58) Danielsson, J.; Jarvet, J.; Damberg, P.; Gräslund, A. *FEBS J.* **2005**, *272*, 3938.
(59) Jarvet, J.; Danielsson, J.; Damberg, P.; Oleszczuk, M.; Gräslund, A. *J. Biomol. NMR* **2007**, *39*, 63.
(60) Hoyer, W.; Grönwall, C.; Jonsson, A.; Ståhl, S.; Härd, T. *Proc. Natl. Acad. Sci. U.S.A.* **2008**, *105*, 5099.
(61) Lindgren, J.; Wahlström, A.; Danielsson, J.; Markova, N.; Ekblad, C.; Gräslund, A.; Abrahmsén, L.; Karlström, A. E.; Wärmländer, S. K. *Protein Sci.* **2010**, *19*, 2319.
(62) Abelein, A.; Lang, L.; Lendel, C.; Gräslund, A.; Danielsson, J. *FEBS Lett.* **2012**, *586*, 3991.
(63) Feng, B. Y.; Toyama, B. H.; Wille, H.; Colby, D. W.; Collins, S. R.; May, B. C.; Prusiner, S. B.; Weissman, J.; Shoichet, B. K. *Nat. Chem. Biol.* **2008**, *4*, 197.